Computational structure-activity relationship (SAR) of berberine analogs in double-stranded and G-quadruplex DNA binding reveals both position and target dependence

Stephanie Sun[1], Bhavesh Ashok[2], Andrew Su[3], Saira Hamid[4], Karthikha Sri Indran[4], Aashi Shah[2], Sarah Su[5], Simrun Sakhrani[6], Edward Njoo[7]

[1]BASIS Independent Silicon Valley, San Jose, California
[2]Amador Valley High School, Pleasanton, California
[3]Foothill High School, Pleasanton, California
[4]Mission San Jose High School, Fremont, California
[5]Los Altos High School, Los Altos, California
[6]The College Preparatory School, Oakland, California
[7]Department of Chemistry, Biochemistry, & Physical Science, Fremont, California

SUMMARY

Berberine, a natural product alkaloid, and its analogs have a wide range of medicinal properties, including antibacterial and anticancer effects. Previous studies showed that berberine and its analogs intercalate into DNA, thereby inhibiting DNA replication. Berberine has also been studied as a photosensitizer and was shown to generate reactive singlet oxygen *in situ*, and this has applications in photodynamic therapy. Various groups have synthesized berberine analogs that have comparable or improved biological activity; however, an exhaustive structure-activity relationship of the free energy of binding of berberine analogs with substitution at C-8, C-12, and C-13 to DNA have not been previously reported. High-throughput virtual screening (HTVS) allows for efficient analysis of compound libraries to identify lead compounds as possible pharmaceutical agents. Here, we employed HTVS towards a library of alkyl or aryl berberine analogs on C-8, C-12, and C-13 to probe binding to double-stranded and G-quadruplex DNA. Predicted free energies of binding to double-stranded DNA and G-quadruplex DNA were generated via molecular docking. The excited state electronic structure calculations were conducted via time-dependent density functional theory to probe the potential photosensitizing activity of each compound, and the potential G-quadruplex stabilizing abilities of key berberine analogs were probed through molecular dynamics simulations on a 4.0 nanosecond timescale. We determined that the nature of the substituent, the position of the substituent, and the nucleic acid target affect the free energy of binding of berberine analogs to DNA and G-quadruplex DNA, however berberine analogs did not result in net stabilization of G-quadruplex DNA.

INTRODUCTION

Berberine (**Figure 1**), a naturally occurring isoquinoline alkaloid extracted from the roots and stem of plants from the genus *Berberis,* has been of great medicinal interest due to its wide range of reported biological activities, including antimicrobial, antidiabetic, and anticancer activity (1-5). Berberine-containing extracts have been used as a medicinal agent in many traditional cultures dating back to 3000 BC (6).

The mechanism of action of berberine is believed to be intercalation with DNA, where it acts as a photosensitizer. Berberine was previously found to intercalate in DNA with a high free energy of binding (ΔG), driven by electrostatic attractions and pi-stack interactions between the compound and nucleotide base pairs in DNA secondary structures (7). Upon photoirradiation of the berberine-DNA complex, berberine acts as a photosensitizer and generates singlet oxygen, a reactive oxygen species, which oxidizes guanines and results in DNA damage, thereby inhibiting DNA replication and halting cell division (8). This was previously studied in application to photodynamic therapy as a potential treatment of various types of cancers and antimicrobial agents (9-10). Berberine has also been reported to stabilize G-quadruplex DNA (G4DNA), a four-stranded, noncanonical secondary structure of DNA consisting of guanine-rich DNA sequences
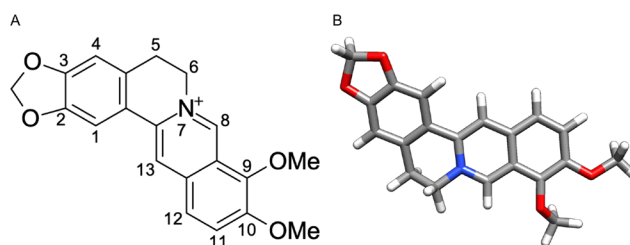

Figure 1. Background and introduction of Berberine 1.
(a) Chemical structure of berberine with the carbons numbered.
(b) 3D structure of berberine (DFT optimized, B3LYP, def2-SVP).

(11). Stabilization of G4DNA inhibits telomerase, an enzyme that is overexpressed in cancers; this inhibition of telomerase results in the inhibition of cancer activity (12).

Several semisynthetic analogs and derivatives of berberine have previously been prepared and evaluated for biological activities; some of these are reported to have comparable or superior antibacterial, antifungal, or anticancer activity compared to the natural product, and some have been reported to possess improved free energies of binding to DNA and G4DNA. Addition of an alkyl or aryl chain to C-8 of berberine can be achieved via nucleophilic addition of alkyl or aryl Grignard; such compounds have been reported to have more potent antimicrobial activity (13), but the possible role of the stereogenic center at C-8 in DNA binding is not yet known (**Figure 2a**). Wang *et al.* previously reported a library of 12-amine-berberine derivates that demonstrate increased anticancer activity compared to berberine (14). The synthesis and biological screening of 13-alkylberberine analogs revealed that the addition of alkyl chains of various lengths

improves the anticancer, anti-inflammatory, and antioxidant activity of berberine (15-16). It has also been reported that a borohydride reduction at the C-8 iminium to yield dihydroberberine generally results in a loss of antimicrobial efficacy (17). While many have studied the biological activities of berberine and its analogs, less than 20 percent of studies reported in the last 10 years quantify the DNA free energy of binding of such analogs, and even fewer have produced crystal structures of berberine bound to a DNA target.

Here, we report an extensive *in silico* virtual screen of a representative library of 8-, 12-, and 13-alkyl and aryl berberine analogs (**Figure 2b**). The use of HTVS, which screens small molecule libraries against potential drug targets, has enabled the rapid and efficient screening of large libraries of chemical entities (18-20). We employed molecular docking to determine the predicted free energy of binding of each analog to each of the two DNA targets and we performed molecular dynamics (MD) simulations on berberine and selected analogs to simulate potential ligand-mediated stabilization
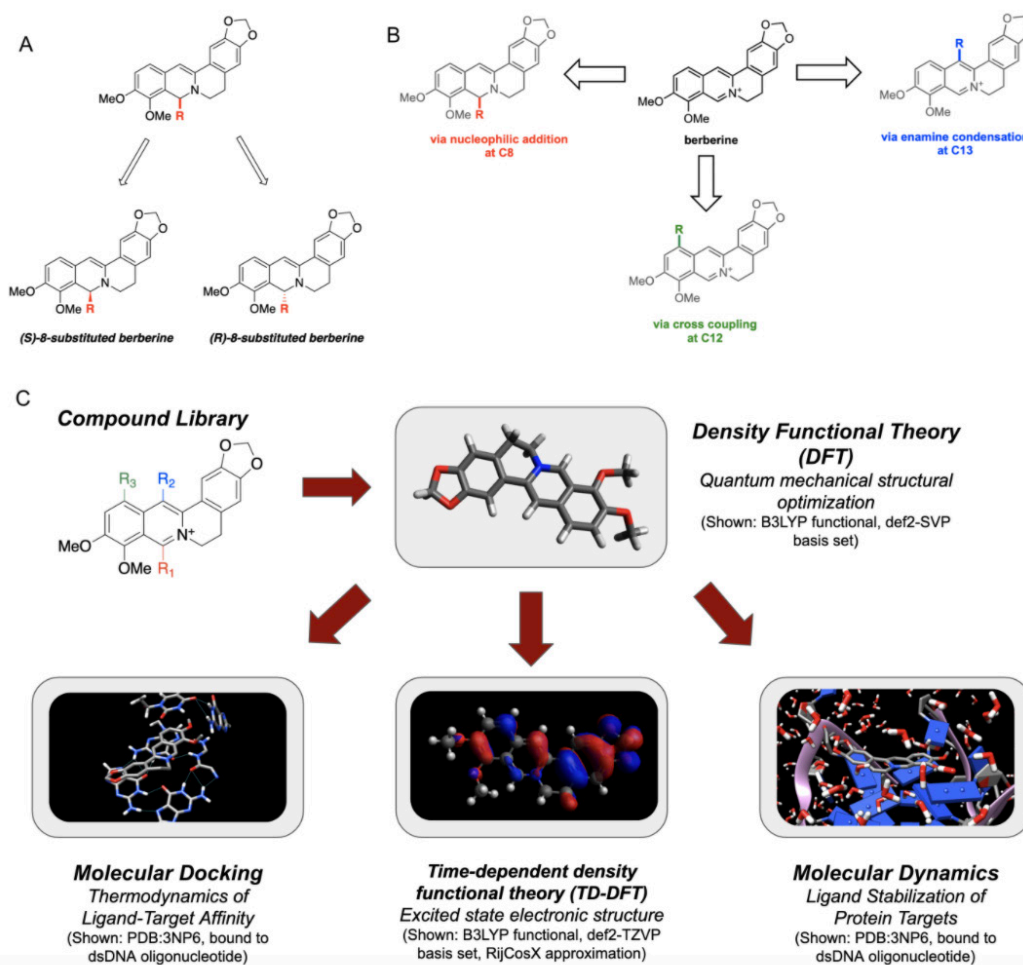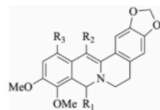

Figure 2. Design of the library of berberine analogs and our methodology in this study. (a) A stereocenter is formed when alkyl and aryl chains are added to C-8 of berberine, resulting in R and S enantiomers. Both R and S enantiomers of all C-8 analogs were studied. **(b)** Possible reactions for the synthesis of C-8, C-12, and C-13 analogs that inspired the design of the library. Possible reactions include a nucleophilic addition to C-8 with Grignard reagents, treatment of berberine with elemental bromine yields 12-bromoberberine, which can serve as a handle for cross coupling reactions, and enamine condensations to C-13. **(c)** Workflow and methodology in our work.

of the G4DNA complex. We implemented time-dependent density functional theory (TD-DFT) calculations to predict the wavelength of maximal absorbance and the relative energies of the singlet and triplet excited states of each analog. The energetic ordering of these excited states affects whether the berberine analogs can generate singlet oxygen, the process of which can result in DNA damage (**Figure 2c**). Since many DNA intercalators rely on pi-stack interactions or electrostatic attractions, we initially hypothesized that the addition of aromatic systems to C-8, C-12, or C-13 would provide an increase in ΔG, and that loss of the cationic iminium at C-8 would diminish the free energy of binding (21).

In this work, we screened a library of 31 berberine analogs against 2 biological targets, double-stranded DNA (dsDNA) d(CGTACG) and G4DNA, based on previously-reported crystal structures (PDB codes 3NP6 for dsDNA and 6JWD for G4DNA) (22-23). The results of the HTVS, MD simulations, and TD-DFT calculations indicate that the impact of aryl and aliphatic substitution on DNA free energy of binding is both position-dependent and target-dependent. We determined that the binding affinity of berberine analogs to dsDNA and G4DNA is affected by the nature and carbon position of the substituent, and these compounds have no net stabilizing effect on G4DNA complexes.
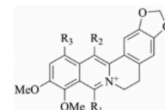
RESULTS

Molecular docking of the library of berberine analogs with dsDNA d(CGTACG) and G4DNA was completed using Autodock Vina (24-25). Docking parameters were determined from previously reported crystal structures, and the high degree of similarity in ligand positioning achieved between docked poses and the crystal structure demonstrates the predictivity of the docking parameters used (22-23). Results were quantified based on the ΔG in kcal/mol (**Figure 3**).

dsDNA Binding

Docking results for analogs with bromo-, phenyl-, and naphthyl- substitutions at the C-12 position had greater ΔG to dsDNA than analogs with substitutions at C-8 and C-13, and some of these compounds exhibited greater ΔG values than berberine itself. A lower ΔG value indicates stronger binding affinity to target proteins, and a negative ΔG indicates that the interaction between the compound and target is thermodynamically stable. Compounds with naphthyl groups on C-12 had a ΔG of -6.0 and -6.8 kcal/mol (**Figure 4c**), compound **12c** and **12d**, respectively. Interestingly, naphthyl additions to the C-8 position yielded lower ΔG values than berberine, with ΔG values of -2.1 and -3.3 kcal/mol for the R and S enantiomers of compound **8h**, respectively. The same trend was seen in the R and S enantiomers of compound **8i**, whose ΔG increased to -1.0 kcal/mol and -2.2 kcal/mol, respectively.

Compound 2, 8a-h

Compound	R_1	R_2	R_3	ΔG - dsDNA	ΔG - G4DNA
2	H	H	H	-6.2	2.5
8a	CH_3	H	H	R = -4.0, S = -4.1	R = -0.1, S = 2.3
8b	C_2H_5	H	H	R = -4.2, S = -3.8	R = 0.8, S = 1.4
8c	C_4H_9	H	H	R = -4.5, S = -4.3	R = 3.3, S = 5.0
8d	C_6H_{13}	H	H	R = -3.8, S = -3.6	R = 3.0, S = 2.5
8e	C_8H_{17}	H	H	R = -3.7, S = -3.6	R = 6.3, S = 1.5
8f	$C_{10}H_{21}$	H	H	R = -3.0, S = -3.2	R = 9.1, S = 3.4
8g	(phenyl)	H	H	R = -4.4, S = -3.4	R = 6.1, S = 9.8
8h	(naphthyl)	H	H	R = -2.1, S = -3.3	R = 9.3, S = 9.2
8i	(naphthyl)	H	H	R = -1.0, S = -2.2	R = 65.9, S = N/A

Compound 1, 12a-d, 13a-g

Compound	R_1	R_2	R_3	ΔG - dsDNA	ΔG - G4DNA
1	H	H	H	-5.6	2.6
12a	H	H	Br	-5.8	4.0
12b	H	H	(phenyl)	-5.9	25.7
12c	H	H	(naphthyl)	-6.0	35.5
12d	H	H	(naphthyl)	-6.8	N/A
13a	H	C_4H_9	H	-4.8	3.2
13b	H	C_6H_{11}	H	-4.8	7.4
13c	H	C_8H_{17}	H	-4.6	4.1
13d	H	$C_{10}H_{21}$	H	-4.3	8.2
13e	H	(alkenyl)	H	-4.4	10.4
13f	H	(phenyl)	H	-4.9	4.9
13g	H	(benzyl)	H	-4.2	11.1

Figure 3. Thermodynamics of the binding of the library berberine analogs to dsDNA and G4DNA. Free energies of binding (ΔG) are reported in kcal/mol and represent the ΔG of the most thermodynamically-stable predicted binding pose.
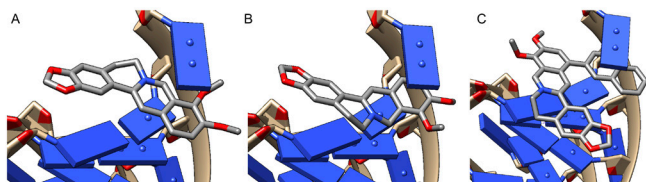
Figure 4. Most thermodynamically stable binding pose of representative compounds in our library to dsDNA. (a) Berberine 1 (ΔG = -5.6 kcal/mol) **(b)** Dihydroberberine 2 (ΔG = -6.2 kcal/mol) **(c)** Compound 12d, the berberine analog with the best free energy of binding to dsDNA (ΔG = -6.8 kcal/mol).

Figure 5. Binding poses of berberine and berberine analogs to G4DNA. (a) Berberine 1 (ΔG = 2.6 kcal/mol) **(b)** Dihydroberberine 2 (ΔG = 2.5 kcal/mol) **(c)** Both enantiomers of compound 8a. The structure in blue is the R enantiomer (ΔG = -0.1 kcal/mol), and the structure in purple is the S enantiomer (ΔG = 2.3 kcal/mol).

G4DNA Binding

Berberine analogs had lower free energies of binding to G4DNA than dsDNA. Unlike dsDNA, aliphatic chains on the C-8 positions demonstrated the best binding affinity to G4DNA. The R enantiomer of compound **8a** had the lowest ΔG value of all analogs screened at -0.1 kcal/mol (**Figure 5c**). Additions of naphthyl groups at both C-8 and C-12 greatly decreased the ΔG values of analogs **8h**, **8i**, **12c**, and **12d** to G4DNA. Compounds **8i** and **12d** were not able to dock to G4DNA. It is unclear why AutoDock Vina returned positive ΔG values for the DNA-berberine binding interaction.

The lengthening of the alkyl chain on the C-8 analogs also resulted in decreased free energy of binding of the compound to G4DNA. This could be attributed to steric clashes, in which members of the alkyl chain past the fourth carbon overlap with atoms of the receptor without taking part in the binding interactions. This is thermodynamically unfavorable due to repulsive electron interactions between these clashing atoms, increasing the ΔG value. Differences were also observed between the R and S enantiomers of these analogs, with thermodynamic favorability of the R enantiomer for alkyl ch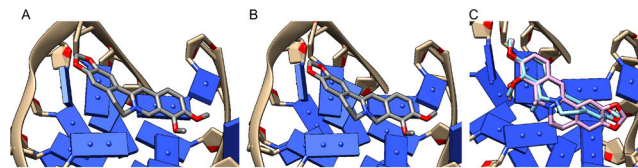ains four carbons and shorter. This trend seems to be reversed for alkyl chains longer than four carbons, with the S enantiomer having lower ΔG values.

Time-Dependent Density Functional Theory

TD-DFT was utilized to study the excited state electronic structure of each compound. Moreover, the molecular orbital energies that resulted allowed us to probe whether berberine analogs could undergo electronic transitions that can effectively produce singlet oxygen (**Figure 6**).

Here, we found that the energy gap generated by berberine and all analogs screened was sufficient for the production of singlet oxygen species. The energy emitted through phosphorescence, the transition from the triplet excited state back to ground state, is transferred to oxygen for the production of singlet oxygen (**Figure 7**). The energy gap necessary for the production of the singlet oxygen is 0.98 eV, which all of our compounds are able to undergo (26). The absorbance maximum wavelengths of the analogs of berberine undergo a blueshift. The C-8 compounds, which contain the reduced isoquinoline chromophore, undergo a larger blueshift than analogs with the same isoquinolinium chromophore as berberine. The rate of intersystem crossing

Compound	E_{S0} (eV)	E_{S1} (eV)	E_{T1} (eV)	$\Delta E_{S0 \to S1}$ (H → L)	$\Delta E_{T1 \to S0}$ (H → L)	λ_{max} (nm)	Compound	E_{S0} (eV)	E_{S1} (eV)	E_{T1} (eV)	$\Delta E_{S0 \to S1}$ (H → L)	$\Delta E_{T1 \to S0}$ (H → L)	λ_{max} (nm)
1	-5.645	-2.701	-3.854	2.944	1.791	421	**12a**	-5.976	-2.851	-4.063	3.125	1.913	397
2	-4.735	-1.119	-2.447	3.616	2.288	343	**12b**	-5.837	-2.700	-3.953	3.137	1.884	396
8a	-4.775	-1.069	-2.400	3.706	2.375	335	**12c**	-5.822	-2.710	-3.942	3.112	1.880	399
8b	-4.768	-1.048	-2.382	3.720	2.396	334	**12d**	-5.718	-2.699	-3.962	3.019	1.756	411
8c	-4.688	-1.123	-2.447	3.565	2.241	348	**13a**	-5.720	-2.610	-3.892	3.110	1.828	399
8d	-4.685	-1.112	-2.430	3.573	2.255	347	**13b**	-5.719	-2.608	-3.892	3.111	1.827	399
8e	-4.861	-1.117	-2.436	3.744	2.425	331	**13c**	-5.725	-2.610	-3.880	3.115	1.845	398
8f	-4.620	-1.030	-2.343	3.590	2.277	346	**13d**	-5.814	-2.584	-3.876	3.230	1.938	384
8g	-4.766	-1.219	-2.506	3.547	2.260	350	**13e**	-5.724	-2.609	-3.893	3.115	1.831	398
8h	-4.771	-1.568	-2.563	3.203	2.208	387	**13f**	-5.814	-2.584	-3.876	3.230	1.938	384
8i	-4.699	-1.487	-2.419	3.212	2.280	386	**13g**	-5.761	-2.665	-3.940	3.096	1.821	401

Figure 6. Energy of the ground state, singlet excited state, and triplet excited state of berberine and its analogs from TD-DFT calculations. Electronic transitions are reported in eV, and the wavelength of maximal absorbance is reported in nanometers. Calculations were performed using the B3LYP/def2-TZVP level of theory.

can be effectively calculated from Fermi's golden rule based on the spin-orbit coupling matrix elements, but this is not easily implemented in TD-DFT calculations in ORCA (27).

MD simulations were used to probe the potential stabilizing effects and stabilization timescale of the binary complexes between G4DNA and berberine, dihydroberberine, and 8-methylberberine. Specifically, stabilization over time of the G4DNA by berberine and the two analogs were calculated in GROMACS (**Figure 8a**), and the average RMSD was calculated over the same time interval (**Figure 8b**). G4DNA with berberine had a lower maximum RMSD value than G4DNA with dihydroberberine and 8-methylberberine. RMSD is a measure of the change in atom position from an initial point to a final point, and a lower RMSD value indicates that an atom or system has moved less from its initial position. A lower RMSD value over time indicates that the complex has been relatively stable. Unpaired t-testing revealed that the differences in RMSD between 8-methylberberine (2-tail unpaired *t*-test, *p*-value 0.10), dihydroberberine (2-tail unpaired *t*-test, *p*-value 0.087), and G4DNA were insignificant at a 95% confidence interval. However, the difference between the RMSD of G4DNA and berberine was statistically significant (2-tail unpaired *t*-test, *p*-value 0.00003), suggesting a destabilization of G4DNA by berberine.

DISCUSSION

Molecular docking, TD-DFT excited state calculations, and molecular dynamics simulations were performed to investigate the SAR in berberine analogs on the impact of aliphatic and aromatic side chains at C-8, 12, and 13 in the free energy of binding towards dsDNA and G4DNA. While the ΔG values of G4DNA appear positive, the results were predictive because the most thermodynamically favorable binding pose was accurately predicted. Analogs with the best free energy of binding to dsDNA were the 12-substituted analogs, which had ΔG values of -5.8 to -6.8 kcal/mol compared to a ΔG of -5.6 kcal/mol for berberine. The aromatic 12-substituted analogs performed the best overall with ΔG values comparable to berberine, likely due to the increased number of pi-stacking interactions.

Contrary to our initial hypothesis, berberine analogs with aromatic substitution did not always have the highest free energy of binding to either dsDNA or G4DNA targets. Rather, the effect of aryl versus aliphatic substitution on DNA binding appears to be dependent on not only the nature of the substituted group, but also the substituted carbon position (C-8, C-12, C-13) and the nucleic acid target, as different trends were observed in ΔG to dsDNA and G4DNA. Moreover, it appears that a loss of the persistent cation in the isoquinolinium core of berberine, as in the case of dihydroberberine and any 8-alkyl or 8-aryl analog, is not necessarily detrimental to DNA binding. Additionally, against initial expectations, MD simulations do not seem to indicate net stabilization of the G-quadruplex-ligand binary complex.
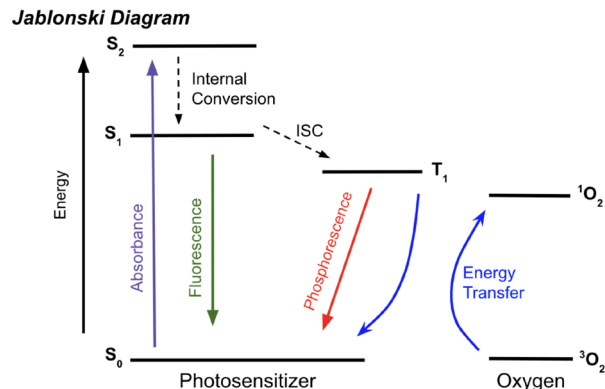

Jablonski Diagram

Figure 7. Jablonski Diagram depicting electronic transitions that occur as photosensitizers excite oxygen into singlet oxygen. Initial absorbance of a photon excites the ground state photosensitizer (S_0) to the second excited state (S_2), which undergoes rapid internal conversion to the first excited state (S_1). This undergoes intersystem crossing (ISC) to the first excited triplet state (T_1), which can excite ground state triplet oxygen ($^3O_2$) to an excited singlet state ($^1O_2$).
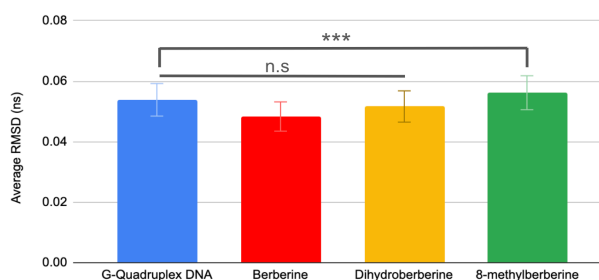
A
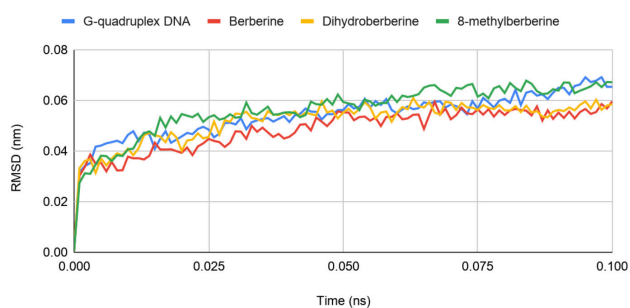
B

Figure 8. Root-mean-square deviation (RMSD) of atomic position calculations from molecular mechanics. (a) Average RMSD of G4DNA, G4DNA with berberine, G4DNA with dihydroberberine, and G4DNA with 8-methylberberine over 0.1 nanosecond in water **(b)** Net Destabilization of G4DNA by berberine, dihydroberberine, and 8-methylberberine. 2-tail unpaired t-testing was completed to determine statistical significance between the average RMSD values of G4DNA compared to G4DNA with berberine, G4DNA with dihydroberberine, and G4DNA with 8-methylberberine. "n.s." indicates that the difference in average RMSD values are not statistically significant (*p*-value >0.05). "****" indicates that the difference in average RMSD values are statistically significant (*p*-value = 0.0001).

Visual analysis of the docked poses suggest that steric effects are operative in the superior ΔG of 8-alkyl berberine analogs in G4DNA (**Figure 3**, compounds **8a**-**8d**). The crystal structure positions the compound in a manner where C-8 directly faces the DNA, forcing a substituent on C-8 to have more interactions with the G4DNA. However, the relatively poor ΔG value of a larger substituent such as the aromatic compound **8g** is potentially caused by greater steric encumbrance to intercalate in G4DNA. Aliphatic 8-substituted analogs in the R enantiomers of G4DNA are more thermodynamically favorable than S enantiomers for four carbons and shorter, which can be explained by reduced steric hindrance in the direction of the S enantiomers.

The analogs with the lowest ΔG to G4DNA and the best ΔG to dsDNA were the aromatic substituents. The lower affinity for aromatic chains in G4DNA can be attributed to the G4DNA complex folding, exacerbating the problems of steric hindrance (28). The larger variation in free energies of binding with G4DNA can be attributed to the smaller binding since bigger molecules, like compound **12b**, are too sterically hindered to bind in more thermodynamically favorable conformer poses.

Compound 8a had the highest ΔG to G4DNA; however, MD simulations revealed that this compound destabilized G4DNA with an average RMSD value of 0.0562 ns while G4DNA has an average RMSD value of 0.0538 ns. Comparatively, berberine and dihydroberberine had much higher stabilization capabilities with average RMSD values of 0.0483 and 0.0516 ns respectively, which are lower than the average G4DNA's RMSD value.

Through TD-DFT calculations, we were able to determine that the berberine analogs can undergo an electronic transition that is sufficient for the production of singlet oxygen. This is deemed to be beyond the current scope of the study. Further studies on the lifetime of the triplet state of the berberine analogs are necessary to accurately understand the photosensitizing ability of berberine. One limitation with the use of berberine analogs is the blueshift observed in the maximum wavelength of absorbance. Many biomolecular entities, such as DNA and aromatic amino acids, have absorbance in the ultraviolet range, and photodynamic therapy with berberine analogs could possibly result in undesired side effects (29).

Through molecular docking, TD-DFT, and MD simulations we present an exhaustive SAR of berberine and its C-8, C-12, and C-13 analogs with respect to their free energy of binding to both dsDNA and G4DNA. While this study primarily focused on computational work and rapid *in silico* screening of such compounds, it provides the basis for future work in the chemical synthesis and *in vitro* evaluation of hit structures and their DNA-binding efficacy.

MATERIALS AND METHODS
Molecular Mechanics Pre-Optimization

Avogadro, a cross-platform molecular editor, was used to create three-dimensional computational models of berberine and each of the studied analogs (30). Prior to density functional theory (DFT) geometry optimization, each model was initially optimized by molecular mechanics using the Merck Molecular Force Field (MMFF94) to 10,000 steps. Input files for DFT structural optimizations were created on Avogadro.

DFT Structural Optimization

Density functional theory (DFT) is a quantum mechanical modelling method based on electron density that is used to calculate the ground state energies of molecules and solids (31). Here, DFT was used to calculate the most quantum mechanically minimized molecular geometries of berberine analogs. ORCA, an *ab initio* quantum mechanical molecular modeling software, was used in tandem with Avogadro to generate ORCA input files to compute the DFT optimized structure of berberine and each analog (32-33). An implicit conductor-like polarizable continuum (CPCM) solvation model of water was used to simulate the conditions of an aqueous environment. B3LYP, a hybrid functional, was chosen for the calculation due to its low computational cost compared to other traditional functionals, as well as its acceptance in the scientific community for creating low parameter, accurate results (34). The def2-SVP basis set was used as the compounds are comprised of light main group elements. All DFT calculations were carried out to default convergence thresholds. Additionally, TD-DFT, with the B3LYP hybrid functional, was used to model and calculate the excited singlet and triplet energies of berberine and its analogs, which is instrumental to understanding the photosensitizing ability of berberine analogs. The def2-TZVP basis set was used in conjunction with the RIJCOSX approximation method to greatly accelerate the calculation with negligible decrease in accuracy and significant reduction of computational expense.

AutoDockTools

AutoDockTools (ADT), a part of the MGLTools suite, is a graphical user interface that allows for the preparation and generation of coordinate files for use in AutoDock Vina (34). To prepare the dsDNA d(CGTACG) and G4DNA moieties for the docking procedure, ADT was used to identify the receptors as a macromolecule, which adds Gasteiger charges to the molecule and merges non-polar hydrogens. The search space for the ligand was also chosen at this stage, modelled after 3NP6 for dsDNA and 6JWD for G4DNA. Each ligand was prepared by importing the coordinate file into ADT as a ligand, upon which the Gasteiger charges were computed and applied to the molecule. The identification of the torsion tree root allowed the number of rotatable bonds to be set, allowing for maximum conformity of the ligand to induce fit into the specified search grid.

AutoDock Vina

AutoDock Vina is an open source molecular docking program, allowing us to understand and model the

thermodynamics of ligand-protein interactions (36). Configuration of Vina included the definition of the search grid from ADT. Additionally, Vina was queried to generate 15 conformers of each ligand rather than the default 9 binding modes in order to avoid omission of possible conformers. The exhaustiveness value of the search was doubled from the default 8 to 16 in order to generate models from more computationally exhaustive methods. The validity of the docking parameters used was first assessed by comparing the predicted highest-affinity binding pose of berberine to dsDNA d(CGTACG) with that which was previously reported in its crystal structure (PDB 3NP6), and these were found to be consistent.

UCSF Chimera/ChimeraX

Visual analysis to determine the accuracy of the computationally determined binding mode of the berberine molecule relative to that of the crystal structure shown in 3NP6 and 6JWD was done in UCSF Chimera and UCSF ChimeraX molecular visualization programs (37-38).

GROMACS

GROMACS, or the GROningen MAchine for Chemical Simulations, is a molecular dynamics (MD) package that simulates interactions between proteins and ligands using Newton's laws of motion (39). GROMACS was used to carry out high-level molecular dynamics simulations to computationally model the interactions between atoms in the most thermodynamically favorable conformers of berberine, dihydroberberine, and G4DNA. The AMBER99SB force field and an explicit TIP3 water solvation model were used. Energy minimization was conducted in order to minimize the structure and remove clashes within the system. An equilibration step was conducted to meet temperature and pressure constraints imposed by the MD simulation. Configuration of the force field using AMBER99SB parametrics and bond-charge correction (BCC) charges on the ligand level was carried out on the ACPYPE Web Server (40). Additional time-dependent RMSD calculations to determine net stabilization of the DNA were also carried out using GROMACS. MDWeb was used to generate the structure of each MD simulated system in the PDB format with GROMACS trajectories for visualization in Chimera (41).

DFT, TD-DFT, molecular docking, and molecular dynamics calculations were performed on a Dell PowerEdge 710 server with a 24 core Intel Xeon X5660 processor at 2.80GHz and 32GB RAM.

Wavelength of Excitation

The minimum energy in electron-volts (eV) to excite berberine and its analogs was found by determining the energy difference between the lowest unoccupied molecular orbital (LUMO) by the highest occupied molecular orbital (HOMO). The wavelength corresponding to the HOMO-LUMO gap was determined according to the following equation:

$$\lambda = \frac{hc}{E} = \frac{(6.626 * 10^{-34} Js)(3.00 * 10^8 m/s) * 10^9 nm/m}{(LUMO - HOMO) * 1.602 * 10^{-19} J/eV}$$

HOMO and LUMO orbitals were visualized on Avogadro. Orbital energies were calculated through time-dependent density functional theory (TD-DFT) calculations in ORCA.

REFERENCES

1. Grycová, Lenka, *et al*. "Quaternary Protoberberine Alkaloids." *Phytochemistry*, vol. 68, no. 2, 2007, pp. 150–175., doi:10.1016/j.phytochem.2006.10.004.

2. Wang, Ye, *et al*. "The Anti-Cancer Mechanisms of Berberine: A Review." *Cancer Management and Research*, Volume 12, 2020, pp. 695–702., doi:10.2147/cmar.s242329.

3. Stermitz, F. R., *et al*. "Synergy in a Medicinal Plant: Antimicrobial Action of Berberine Potentiated by 5'-Methoxyhydnocarpin, a Multidrug Pump Inhibitor." *Proceedings of the National Academy of Sciences*, vol. 97, no. 4, 2000, pp. 1433–1437., doi:10.1073/pnas.030540597.

4. Wang, Haoran, *et al*. "Metformin and Berberine, Two Versatile Drugs in Treatment of Common Metabolic Diseases." *Oncotarget*, vol. 9, no. 11, 2017, pp. 10135–10146., doi:10.18632/oncotarget.20807.

5. Lau, Chi-Wai, *et al*. "Cardiovascular Actions of Berberine." *Cardiovascular Drug Reviews*, vol. 19, no. 3, 2006, pp. 234–244., doi:10.1111/j.1527-3466.2001.tb00068.x.

6. Tillhon, Micol, *et al*. "Berberine: New Perspectives for Old Remedies." *Biochemical Pharmacology*, vol. 84, no. 10, 2012, pp. 1260–1267., doi:10.1016/j.bcp.2012.07.018.

7. Krey, A. K., and F. E. Hahn. "Berberine: Complex with DNA." *Science*, vol. 166, no. 3906, 1969, pp. 755–757., doi:10.1126/science.166.3906.755.

8. Hirakawa, Kazutaka, *et al*. "The Mechanism of Guanine Specific Photooxidation in the Presence of Berberine and Palmatine: Activation of Photosensitized Singlet Oxygen Generation through DNA-Binding Interaction." *Chemical Research in Toxicology*, vol. 18, no. 10, 2005, pp. 1545–1552., doi:10.1021/tx0501740.

9. Callaghan, Susan, and Mathias O. Senge. "The Good, the Bad, and the Ugly – Controlling Singlet Oxygen through Design of Photosensitizers and Delivery Systems for Photodynamic Therapy." *Photochemical & Photobiological Sciences*, vol. 17, no. 11, 2018, pp. 1490–1514., doi:10.1039/c8pp00008e.

10. Ragàs, Xavier, *et al*. "Singlet Oxygen in Antimicrobial Photodynamic Therapy: Photosensitizer-Dependent Production and Decay in E. Coli." *Molecules*, vol. 18, no. 3, 2013, pp. 2712–2725., doi:10.3390/molecules18032712.

11. Moraca, Federica, *et al*. "Ligand Binding to Telomeric G-Quadruplex DNA Investigated by Funnel-Metadynamics Simulations." *Proceedings of the National Academy of Sciences*, vol. 114, no. 11, 2017, doi:10.1073/pnas.1612627114.

12. Spiegel, Jochen, *et al*. "The Structure and Function of DNA G-Quadruplexes." *Trends in Chemistry*, vol. 2, no. 2, 2020, pp. 123–136., doi:10.1016/j.trechm.2019.07.002.

13. Iwasa, Kinuko, *et al*. "Antimicrobial Activity of 8-Alkyl- and 8-Phenyl-Substituted Berberines and Their 12-Bromo Derivatives." *Journal of Natural Products*, vol. 61, no. 9, 1998, pp. 1150–1153., doi:10.1021/np980044+.

14. Wang, Bo, *et al*. "Syntheses and Structure–Activity Relationships in Growth Inhibition Activity against Human Cancer Cell Lines of 12 Substituted Berberine Derivatives." *Molecules*, vol. 25, no. 8, 2020, p. 1871., doi:10.3390/molecules25081871.

15. Lee, Dong-Ung, *et al*. "Effects of 13-Alkyl-Substituted Berberine Alkaloids on the Expression of COX-II, TNF-α, INOS, and IL-12 Production in LPS-Stimulated Macrophages." *Life Sciences*, vol. 73, no. 11, 2003, pp. 1401–1412., doi:10.1016/s0024-3205(03)00435-1.

16. Zhang, Lei, *et al*. "Synthesis and Cytotoxicity Evaluation of 13-n-Alkyl Berberine and Palmatine Analogues as Anticancer Agents." *Molecules*, vol. 17, no. 10, 2012, pp. 11294–11302., doi:10.3390/molecules171011294.

17. Rodrigues, Catarina A. B., *et al*. "Synthesizing a Berberine Derivative and Evaluating Antimicrobial Activity To Reinforce with Students the Potential Significance of Small Chemical Structure Changes for Biological Systems." *Journal of Chemical Education*, vol. 95, no. 3, 2018, pp. 492–495., doi:10.1021/acs.jchemed.7b00458.

18. Dhasmana, Anupam, *et al*. "High-Throughput Virtual Screening (HTVS) of Natural Compounds and Exploration of Their Biomolecular Mechanisms." *New Look to Phytomedicine*, 2019, pp. 523–548., doi:10.1016/b978-0-12-814619-4.00020-3.

19. Kumari, Madhulata, *et al*. "High Throughput Virtual Screening to Identify Novel Natural Product Inhibitors for MethionyltRNA-Synthetase of Brucella Melitensis." *Bioinformation*, vol. 13, no. 1, 2017, pp. 8–16., doi:10.6026/97320630013008.

20. Kontoyianni, Maria. "Docking and Virtual Screening in Drug Discovery." *Methods in Molecular Biology Proteomics for Drug Discovery*, 2017, pp. 255–266., doi:10.1007/978-1-4939-7201-2_18.

21. Mignon, P. "Influence of the π-π Interaction on the Hydrogen Bonding Capacity of Stacked DNA/RNA Bases." *Nucleic Acids Research*, vol. 33, no. 6, 2005, pp. 1779–1789., doi:10.1093/nar/gki317.

22. Ferraroni, Marta, *et al*. "X-Ray Diffraction Analyses of the Natural Isoquinoline Alkaloids Berberine and Sanguinarine Complexed with Double Helix DNA d(CGTACG)." *Chemical Communications*, vol. 47, no. 17, 2011, p. 4917., doi:10.1039/c1cc10971e.

23. Wang, Fei, *et al*. "Colchicine Selective Interaction with Oncogene RET G-Quadruplex Revealed by NMR." *Chemical Communications*, vol. 56, no. 14, 2020, pp. 2099–2102., doi:10.1039/d0cc00221f.

24. Morris, Garrett M., *et al*. "AutoDock4 And AutoDockTools4: Automated Docking with Selective Receptor Flexibility." *Journal of Computational Chemistry*, vol. 30, no. 16, 2009, pp. 2785–2791., doi:10.1002/jcc.21256.

25. Trott, Oleg, and Arthur J. Olson. "AutoDock Vina: Improving the Speed and Accuracy of Docking with a New Scoring Function, Efficient Optimization, and Multithreading." *Journal of Computational Chemistry*, 2009, doi:10.1002/jcc.21334.

26. Derosa, M. "Photosensitized Singlet Oxygen and Its Applications." *Coordination Chemistry Reviews*, vol. 233-234, 2002, pp. 351–371., doi:10.1016/s0010-8545(02)00034-6.

27. Alberto, Marta Erminia, *et al*. "Rational Design of Modified Oxobacteriochlorins as Potential Photodynamic Therapy Photosensitizers." *International Journal of Molecular Sciences*, vol. 20, no. 8, 2019, p. 2002., doi:10.3390/ijms20082002.

28. Ida, Jeunice, *et al*. "G-Quadruplexes as An Alternative Recognition Element in Disease-Related Target Sensing." *Molecules*, vol. 24, no. 6, 2019, p. 1079., doi:10.3390/molecules24061079.

29. Schmid, Franz-Xaver. "Biological Macromolecules: UV-Visible Spectrophotometry." *Encyclopedia of Life Sciences*, 2001, doi:10.1038/npg.els.0003142.

30. Hanwell, Marcus D, *et al*. "Avogadro: an Advanced

Semantic Chemical Editor, Visualization, and Analysis Platform." *Journal of Cheminformatics*, vol. 4, no. 1, 2012, doi:10.1186/1758-2946-4-17.

31. Neese, Frank. "The ORCA Program System." *WIREs Computational Molecular Science*, vol. 2, no. 1, 2011, pp. 73–78., doi:10.1002/wcms.81.

32. Lee, Chengteh, *et al*. "Development of the Colle-Salvetti Correlation-Energy Formula into a Functional of the Electron Density." *Physical Review B*, vol. 37, no. 2, 1988, pp. 785–789., doi:10.1103/physrevb.37.785.

33. Kohn, W., *et al*. "Density Functional Theory of Electronic Structure." *The Journal of Physical Chemistry*, vol. 100, no. 31, 1996, pp. 12974–12980., doi:10.1021/jp960669l.

34. Becke, Axel D. "Density-Functional Thermochemistry. III. The Role of Exact Exchange." *The Journal of Chemical Physics*, vol. 98, no. 7, 1993, pp. 5648–5652., doi:10.1063/1.464913.

35. Morris, Garrett M., *et al*. "AutoDock4 And AutoDockTools4: Automated Docking with Selective Receptor Flexibility." *Journal of Computational Chemistry*, vol. 30, no. 16, 2009, pp. 2785–2791., doi:10.1002/jcc.21256.

36. Trott, Oleg, and Arthur J. Olson. "AutoDock Vina: Improving the Speed and Accuracy of Docking with a New Scoring Function, Efficient Optimization, and Multithreading." *Journal of Computational Chemistry*, 2009, doi:10.1002/jcc.21334.

37. Pettersen, Eric F., *et al*. "UCSF Chimera - A Visualization System for Exploratory Research and Analysis." *Journal of Computational Chemistry*, vol. 25, no. 13, 2004, pp. 1605–1612., doi:10.1002/jcc.20084.

38. Goddard, Thomas D., *et al*. "UCSF ChimeraX: Meeting Modern Challenges in Visualization and Analysis." *Protein Science*, vol. 27, no. 1, 2017, pp. 14–25., doi:10.1002/pro.3235.

39. "GROMACS." *Gromacs*, www.gromacs.org/.

40. Silva, Alan W Sousa Da, and Wim F Vranken. "ACPYPE - AnteChamber PYthon Parser InterfacE." *BMC Research Notes*, vol. 5, no. 1, 2012, p. 367., doi:10.1186/1756-0500-5-367.

41. Hospital, Adam, *et al*. "MDWeb and MDMoby: an Integrated Web-Based Platform for Molecular Dynamics Simulations." *Bioinformatics*, vol. 28, no. 9, 2012, pp. 1278–1279., doi:10.1093/bioinformatics/bts139.